RSC Advances

PAPER

View Article Online
View Journal | View Issue

Cite this: *RSC Adv.*, 2019, **9**, 21438

Rational design of functionalized covalent organic frameworks and their performance towards CO_2 capture†

Shuhao An, Ting Xu, Changjun Peng,* Jun Hu and Honglai Liu*

Received 9th May 2019
Accepted 2nd July 2019

DOI: 10.1039/c9ra03487k

rsc.li/rsc-advances

We describe the design and synthesis of two new functionalized covalent organic frameworks, named Cz-COF and Tz-COF, by using monomers containing carbazole and benzobisthiazole as building blocks. The resultant materials possess high crystallinity, permanent porosities as well as abundant heteroatom activated sites in the framework. As solid adsorbents, both COFs exhibit excellent CO_2 uptake (11.0 wt% for Cz-COF and 15.4 wt% for Tz-COF), high adsorption selectivity for CO_2 over N_2 and good recyclability.

Introduction

Covalent organic frameworks (COFs)[1] with periodically ordered structures are a new emerging type of porous crystalline material, and have gained great attention in recent years.[2–4] Owing to their features of robust framework, inherent porosity and tailor-made functionalities, COFs have recently been seen as a new porous platform for extensive applications such as gas storage and separation,[5–7] optoelectronics,[8–10] catalysis,[11–13] and chemical sensor.[14–16] Thus far, in order to achieve excellent performance, a pore channel post-modification strategy has been seen as an effective means of introducing various functional moieties to modify the surface properties of the COF skeleton.[17–20] However, this method tends to reduce the intrinsic porosity and crystallinity of the materials aiming to afford a high density of functional groups, and also suffers from the cleavage of grafted parts during recycling. Correspondingly, the direct construction of functionalized COFs by pre-designed monomers will reduce multistep synthetic procedure and allow the *in situ* introduced active sites to be more evenly dispersed in the framework.[21,22] Due to the solubility and geometric symmetry of building blocks have to be taken into account, the development of functionalized COFs still remains difficult and it is therefore strongly desired based on this method.

On the other hands, with rapid industrialization development and the progress of human society, the continuous emission of carbon dioxide (CO_2) in the atmosphere has become a massive global problem. For this reason, developing effective technologies and strategies to effectively capture CO_2 and alleviate this predicament is both challenging and urgent.[23] Carbon capture and sequestration (CCS) technology is considered an economical and effective way to mitigate the trend of global warming.[24–27] The development of novel nanoporous materials like metal–organic frameworks (MOFs)[28] and porous organic polymers (POPs),[29,30] has shown particular promise for CCS because of their cost-effective physical adsorption process, high efficiency and facile recyclability. Remarkably, various CO_2-philic moieties including triazine,[31] carbazole[32] or benzothiazole[33] have been incorporated into the polymeric networks to enhance the interaction between the material surfaces and CO_2 molecules, consequently exhibiting excellent performance towards CO_2 capture. Thus, rationally design and synthesis of functionalized COFs consist of these moieties not only extend the library of COFs but also investigate COF-based adsorbents for efficient CO_2 capture.

Herein, we contribute to describe the synthesis and CO_2 gas adsorption properties of two new functionalized COFs, Cz-COF and Tz-COF, prepared by using monomers containing carbazole (Cz) and benzobisthiazole (Tz) as building blocks. The crystalline structures and porous properties of obtained COFs are systematically examined through powder X-ray diffraction and nitrogen adsorption–desorption experiments. Most importantly, because of their permanent porosities and abundant heteroatom (N or S) polar sites, both COFs show excellent CO_2 uptake, high adsorption selectivity for CO_2 over N_2 and good recyclability at ambient conditions.

Results and discussion

Although monomers containing Cz and Tz were employed as the scaffolds for the construction of amorphous POPs towards applications such as CO_2 adsorption[33,34] and semiconductor materials,[35] to the best of our knowledge, no previous example of crystalline COFs based on Cz and Tz has been reported. As shown in Scheme 1, our strategy for preparing functionalized COFs involves imine-bond formation reactions together with

State Key Laboratory of Chemical Engineering and School of Chemistry & Molecular Engineering, East China University of Science and Technology, Shanghai, 200237, China. E-mail: cjpeng@ecust.edu.cn; hlliu@ecust.edu.cn

† Electronic supplementary information (ESI) available. See DOI: 10.1039/c9ra03487k

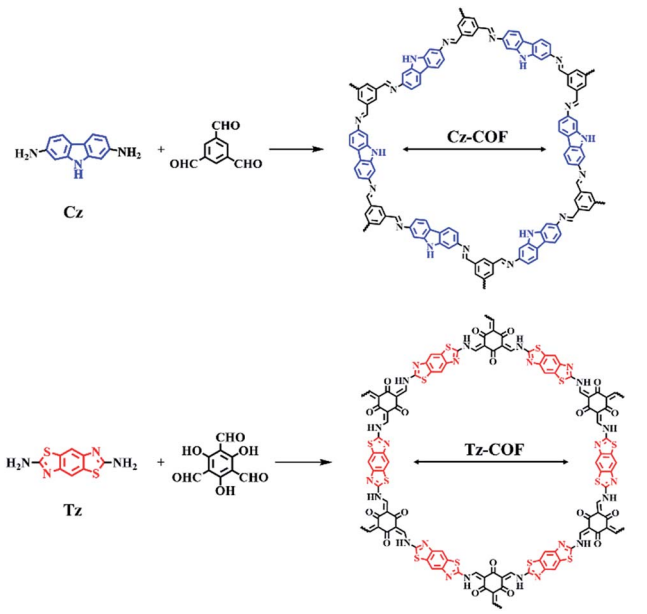

Scheme 1 Schematic representation of the synthesis of functionalized COFs.

typical [C_3 + C_2] schemes. After screening reaction conditions, Cz-COF was synthesized in dioxane/mesitylene/3 M AcOH (15/15/2 v/v) at 120 °C for 3 days and obtained as yellow solid in 85% isolated yield. Tz-COF was synthesized in dioxane/3 M AcOH (5/1 v/v) at 120 °C for 3 days and obtained as red solid in 84% isolated yield. These solid products were insoluble in water and common organic solvents such as tetrahydrofuran (THF), *N*,*N*-dimethylformamide (DMF) and dimethyl sulfoxide (DMSO). Thermogravimetric analysis (TGA) further revealed that both COFs exhibited high thermal stability up to 400 °C (Fig. S3†).

The molecular structures of Cz-COF and Tz-COF were confirmed by Fourier transform infrared (FT-IR) spectroscopy and cross-polarization magic angle spinning (CP-MAS) ^{13}C NMR spectroscopy. In the IR spectrum of Cz-COF (Fig. S4†), the strong absorption peaks for N–H (3405 cm^{-1}) and C–N (1234 cm^{-1}) indicated the presence of the carbazole moiety within the network, while a new characteristic stretching band for C=N (1629 cm^{-1}) was observed.[36] The IR spectrum of Tz-COF (Fig. S5†) indicated total consumption of the monomer based on the disappearance of the N–H absorption peaks of Tz. Moreover, a strong peak at 1596 cm^{-1} arising from the C=C stretching band present in the keto form. It should be noted that the C=O peak of Tz-COF were merged with the C=C stretching band at 1596 cm^{-1} as reported TpPa-1 and TpPa-2 COF.[37] ^{13}C NMR spectrum of functionalized COFs also revealed the structures of their polymeric architectures very well (Fig. S6 and S7†). For Cz-COF, the peak at *ca.* 157 ppm corresponds to the carbon of the imine bonds (C=N). The two peaks at *ca.* 110 ppm and 99 ppm in Cz-COF arise from the phenyl carbons *ortho* to the carbazole nitrogen substitution site.[34] The Tz-COF in keto form was also confirmed by the peak at *ca.* 180 ppm ascribed to typical ketone carbon (C=O). The phenyl carbons from the benzobisthiazole were located at *ca.* 144 ppm and 128 ppm.[33] The morphology of functionalized COFs was examined by scanning electron microscopy (SEM), in which Cz-COF and Tz-COF exhibited different morphology: Cz-COF possessed spherical particle aggregation, whereas Tz-COF showed a large quantity of uniform nanofibers (Fig. S8†).

The powder X-ray diffraction (PXRD) analysis was subsequently used to investigate the crystallinity of the as-synthesized two COFs (Fig. 1). Cz-COF exhibited an intense peak at 3.6° and other three minor peaks at 6.4°, 7.4° and 9.7°, which correspond to the reflection from the (100), (110), (200) and (210) planes, respectively (Fig. 1a, red dot). The periodicity of the 2D sheets as a result of π–π interaction can also be inferred from the broad peak at *ca.* 26.9°, which is ascribed to the reflection from (001) plane.[38] The diffraction pattern of Tz-COF exhibited signals at 3.8°, 6.2°, 7.2°, 9.6° and 26.7° that were assigned to the (100), (110), (200), (210) and (001) planes, respectively (Fig. 1c, red dot). Two types of extended structures based on eclipsed (AA) and staggered (AB) stacking models in the space group *P*6 were generated for both COFs by the Materials Studio software package and then simulated their powder PXRD patterns (Fig. 1a and c, pink and green curve, respectively). The calculated PXRD patterns based on AA stacking model shows excellent agreement with experimental results in terms of peak positions and intensities for both COFs (Fig. 1a and c, blue curve). The Pawley refinements were further conducted and yielded the unit cell parameters with good agreement factors ($a = b = 28.79$ Å, $c = 3.51$ Å, $R_{WP} = 5.63\%$, $R_P = 3.30\%$ for Cz-COF and $a = b = 28.55$ Å, $c = 3.78$ Å, $R_{WP} = 4.79\%$, $R_P = 9.23\%$ for Tz-COF). On the basis of these results, Fig. 1b and d illustrate the eclipsed AA stacking structures of Cz-COF and Tz-COF, respectively.

To investigate the permanent porosities of the functionalized COFs, nitrogen gas adsorption–desorption isotherms were measured at 77 K. The fresh sample was degassed at 120 °C and 1×10^{-5} Torr for 12 h prior to porosity measurement. As shown in Fig. 2, activated Cz-COF and Tz-COF show a sharp uptake under low relative pressure, which reflects the presence of micropores. The step observed at P/P_0 = 0.10–0.20 indicates pore condensation in mesopores with a narrow distribution.[39] The Brunauer–Emmett–Teller (BET) surface areas of the activated COFs were calculated to be 871 $m^2\ g^{-1}$ for Cz-COF and 1439 $m^2\ g^{-1}$ for Tz-COF. The total pore volumes were evaluated at $P/P_0 = 0.99$ to be $V_p = 0.72\ cm^3\ g^{-1}$ for Cz-COF and 1.18 $cm^3\ g^{-1}$ for Tz-COF. The pore size distributions (PSD) based on the nonlocal density functional theory (NLDFT) exhibit two dominant pore diameters of 1.2 nm and 2.0 nm for Cz-COF; 0.7 nm and 2.1 nm for Tz-COF (Fig. 2, insets). The difference between the PSD results with pore width predicted from the eclipsed AA stacking model (2.3 nm for Cz-COF; 2.6 nm for Tz-COF) mainly due to imperfect solid-state stacking of the two-dimension (2D) sheets in the framework that cannot be identified by PXRD studies as reported for many 2D COFs.[40,41]

In view of the fact that the functionalized COFs possess ordered structures, excellent porous characteristics, and *in situ* abundant CO_2-philic heteroatom (N or S) sites among the pore wall, which promote us to investigate their CO_2 uptake capacities. The CO_2 adsorption isotherms were measured up to 1 bar

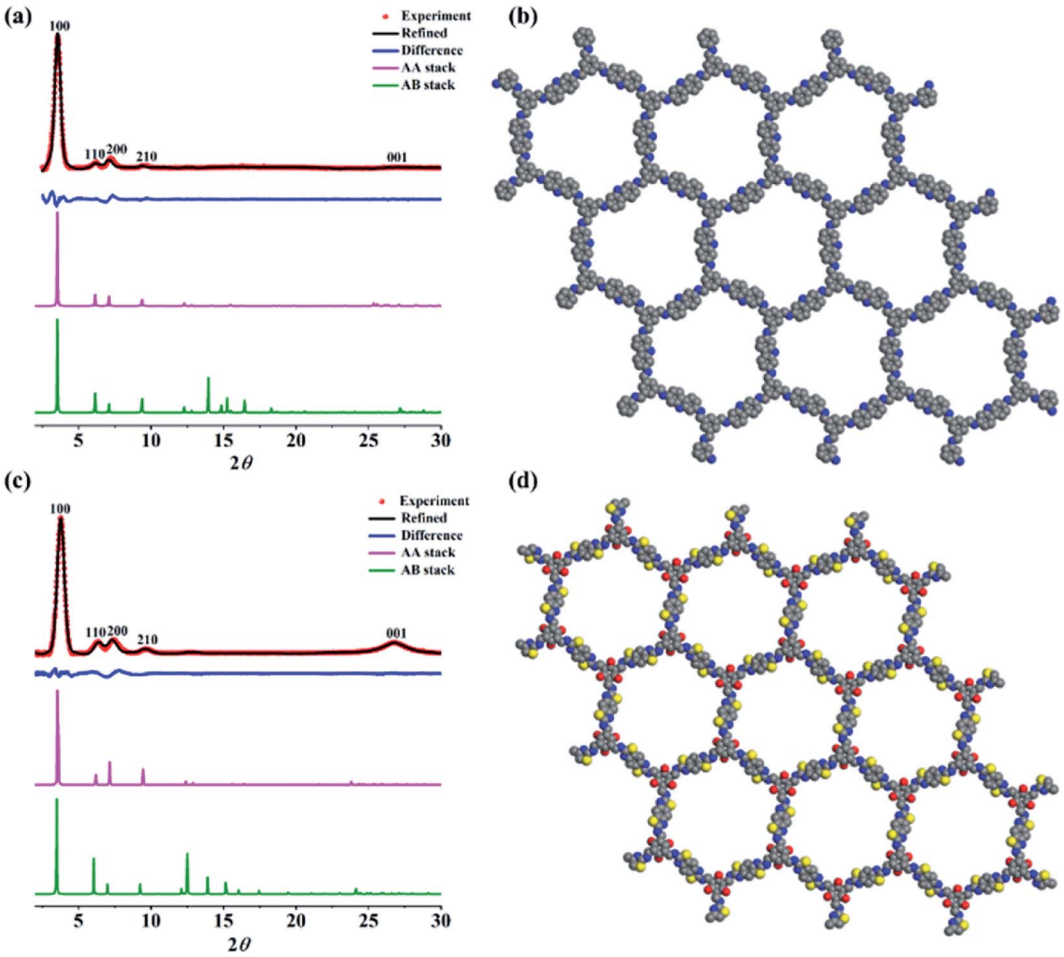

Fig. 1 PXRD patterns of (a) Cz-COF and (c) Tz-COF: experimental (red), Pawley refined (black), difference between experimental and calculated data (blue), calculated for AA-stacking (pink), and calculated for AB-stacking (green). Space filling models of the (b) Cz-COF and (d) Tz-COF in AA.

at both 273 K and 298 K for both COFs (Fig. 3a and b). Remarkably, Cz-COF and Tz-COF show uptakes of 2.5 mmol g^{-1} (11.0 wt%) and 3.5 mmol g^{-1} (15.4 wt%), respectively, at 273 K (Table 1). The CO_2 adsorption capacity of Tz-COF is not only higher than that of many previously reported COFs such as COF-103 (7.6 wt%, S_{BET} = 3530 m^2 g^{-1}),[5] ILCOF-1 (6.0 wt%, S_{BET} = 2723 m^2 g^{-1})[42] and TDCOF-5 (9.2 wt%, S_{BET} = 2497 m^2 g^{-1})[43] even though they have a much higher surface area, but also comparable to the reported excellent amorphous porous organic polymers like benzimidazole-linked polymers BILP-1 (18.8 wt%),[44] microporous polycarbazole CPOP-1 (21.2 wt%)[32] and microporous polyaminal networks PAN-2 (17.7 wt%)[45] under the same conditions (Table S1†). Previous work has shown that heteroatom sites may have an important influence

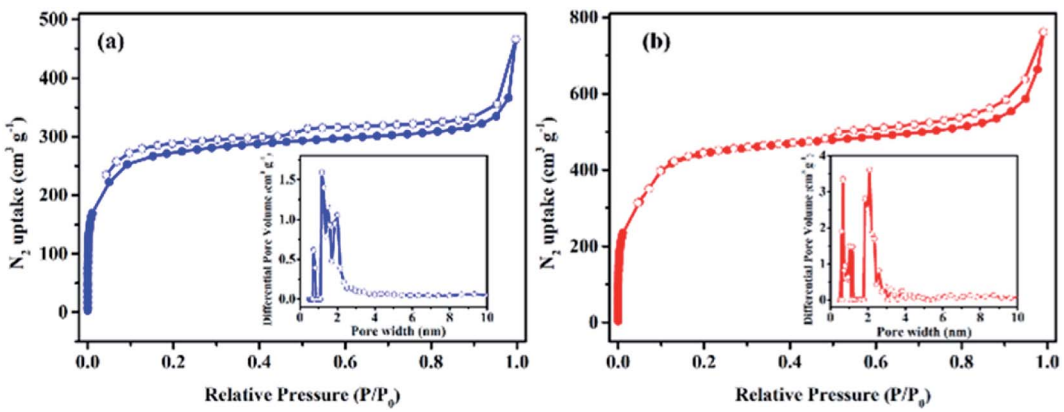

Fig. 2 Nitrogen gas adsorption and desorption isotherms for (a) Cz-COF and (b) Tz-COF. Insets: pore size distributions.

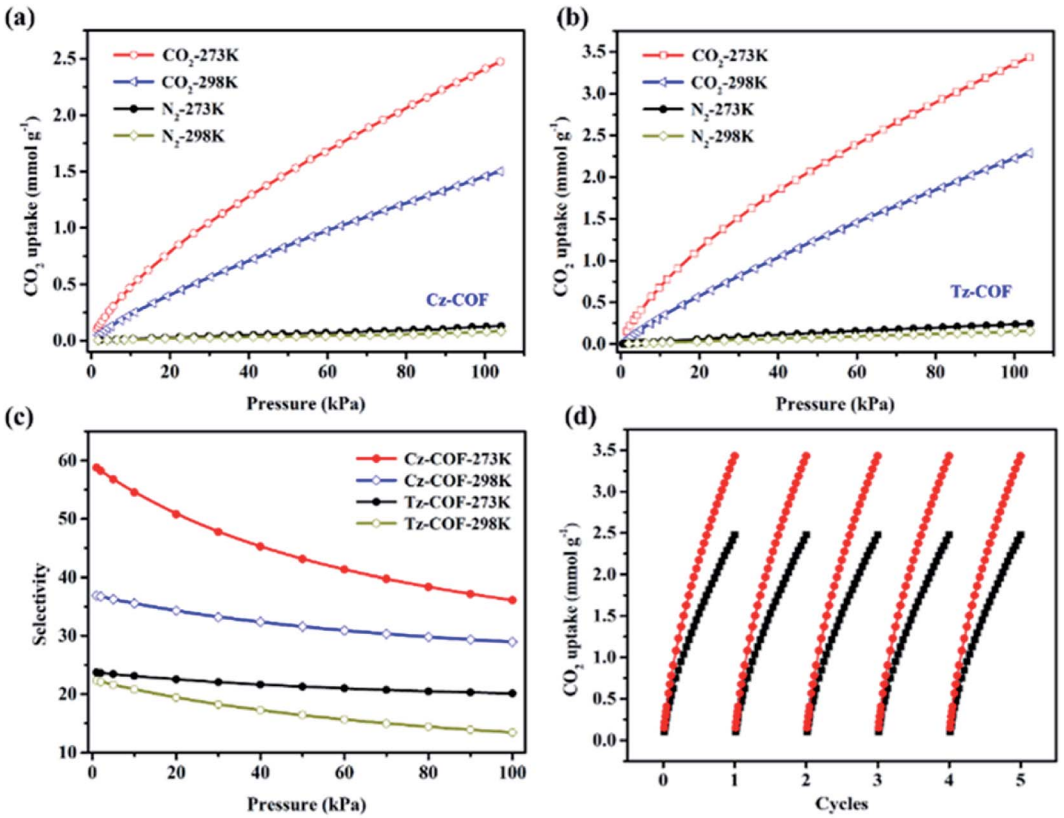

Fig. 3 CO_2 and N_2 adsorption isotherms for (a) Cz-COF and (b) Tz-COF measured at 273 K and 298 K, respectively. (c) The selectivity of functionalized COFs for CO_2 over N_2 obtained from the IAST method. (d) Cyclic CO_2 adsorption for functionalized COFs (black line, Cz-COF; red line, Tz-COF).

on CO_2 adsorption besides the contribution of porous properties.[46] To obtain a better understanding, we then calculated the isosteric heats of adsorption (Q_{st}) for both functionalized COFs by fitting the CO_2 adsorption isotherms obtained from different temperature and applying the Clausius–Clapeyron equation (Fig. S9†). At low adsorption values, Q_{st} was calculated to be 20 kJ mol^{-1} for Cz-COF and 22 kJ mol^{-1} for Tz-COF, suggesting a strong dipole–quadrupole interaction between the COFs framework and CO_2 molecules, which is similar to reported functionalized POPs[32] and COFs.[41]

The selectivity is another key parameter for COF-based adsorbents in gas separation field. We subsequently performed the N_2 adsorption at both 273 and 298 K (1 bar) to examine the selective adsorption for CO_2 over N_2 (Fig. 3a and b). On the basis of Ideal Adsorption Solution Theory (IAST) method,[47] the CO_2/N_2 (10 : 85 v : v) selectivity for the functionalized COFs were calculated to be 36 for Cz-COF and 20 for Tz-COF at 273 K and 1 bar (Fig. 3c). This value of Cz-COF surpasses reported TpPa-COF (32)[48] or $[EtNH_2]_{50}$-H_2P-COF (17)[18] and is lower than the high values of micorporous organic polymers including azo-linked polymer azo-POP-2 (130),[49] aromatic heterocyclic polymer Py-1 (117)[50] and PPN-6-SO_3H (150, 295 K)[51] (Table S1†). At 298 K, the CO_2/N_2 selectivity for Cz-COF and Tz-COF decrease to 29 and 13, respectively. Moreover, the selectivity values for the functionalized COFs were further calculated to be 44 for Cz-COF and 24 for Tz-COF at 273 K using the ratio of the initial slopes of the CO_2 and N_2 adsorption isotherms (Fig. S10†), which is consistent with those obtained from IAST method. Interestingly, at 298 K, the CO_2/N_2 selectivity of Cz-COF and Tz-COF remain at a good level and reach 28 and 21, respectively. Furthermore, five times adsorption–desorption cycle was performed to test the recyclability of the functionalized COFs. As shown in Fig. 3d, there was no apparent loss of uptake amount in each cycling test for both COFs, revealing the good sustainability for functionalized COFs in CO_2 capture process.

Table 1 The characteristics of functionalized COFs in this work

COFs	S_{BET} (m^2 g^{-1})	V_{total}[a] (cm^3 g^{-1})	CO_2 uptake[b] (mmol g^{-1}) 273 K/298 K	Q_{st} (kJ mol^{-1})	Selectivity[c] 273 K/298 K
Cz-COF	871	0.72	2.5/1.5	20	36/28
Tz-COF	1439	1.18	3.5/2.3	22	20/12

[a] Total volumes calculated at $P/P_0 = 0.99$. [b] Measured at the pressure of 1 bar. [c] IAST selectivity (1 bar) for CO_2/N_2 (10 : 85 v : v).

Conclusions

In conclusion, we have synthesized two new functionalized COFs, Cz-COF and Tz-COF, by using monomers containing carbazole and benzobisthiazole as building blocks. Due to their characterization of high crystallinity, permanent porosities as well as abundant heteroatom activated sites in the framework, both COFs exhibit excellent CO_2 uptake (11.0 wt% for Cz-COF and 15.4 wt% for Tz-COF), high adsorption selectivity for CO_2 over N_2 and good recyclability. We expect that these two functionalized COFs successfully prepared in this study not only extend the library of COFs but also inspire us to investigate their potential application in semiconductor material and photocatalyst.

Conflicts of interest

There are no conflicts to declare.

Acknowledgements

The research was supported by the National Natural Science Foundation of China (no. 91334203, 21476070) and the 111 Project of Ministry of Education of China (no. B08021).

Notes and references

1 A. P. Cote, A. I. Benin, N. W. Ockwig, M. O'keeffe, A. J. Matzger and O. M. Yaghi, *Science*, 2005, **310**, 1166–1170.
2 X. Feng, X. Ding and D. Jiang, *Chem. Soc. Rev.*, 2012, **41**, 6010–6022.
3 S. Y. Ding and W. Wang, *Chem. Soc. Rev.*, 2013, **42**, 548–568.
4 M. S. Lohse and T. Bein, *Adv. Funct. Mater.*, 2018, **28**, 1705553.
5 H. Furukawa and O. M. Yaghi, *J. Am. Chem. Soc.*, 2009, **131**, 8875–8883.
6 Y. Zeng, R. Zou and Y. Zhao, *Adv. Mater.*, 2016, **28**, 2855–2873.
7 Y. Pramudya and J. L. Mendoza-Cortes, *J. Am. Chem. Soc.*, 2016, **138**, 15204–15213.
8 S. Wan, J. Guo, J. Kim, H. Ihee and D. Jiang, *Angew. Chem., Int. Ed.*, 2008, **120**, 8958–8962.
9 X. Feng, L. Liu, Y. Honsho, A. Saeki, S. Seki, S. Irle, Y. Dong, A. Nagai and D. Jiang, *Angew. Chem., Int. Ed.*, 2012, **124**, 2672–2676.
10 M. Dogru and T. Bein, *Chem. Commun.*, 2014, **50**, 5531–5546.
11 S. Y. Ding, J. Gao, Q. Wang, Y. Zhang, W. G. Song, C. Y. Su and W. Wang, *J. Am. Chem. Soc.*, 2011, **133**, 19816–19822.
12 Q. Fang, S. Gu, J. Zheng, Z. Zhuang, S. Qiu and Y. Yan, *Angew. Chem., Int. Ed.*, 2014, **126**, 2922–2926.
13 S. Lu, Y. Hu, S. Wan, R. McCaffrey, Y. Jin, H. Gu and W. Zhang, *J. Am. Chem. Soc.*, 2017, **139**, 17082–17088.
14 W. Li, C. X. Yang and X. P. Yan, *Chem. Commun.*, 2017, **53**, 11469–11471.
15 S. Y. Ding, M. Dong, Y. W. Wang, Y. T. Chen, H. Z. Wang, C. Y. Su and W. Wang, *J. Am. Chem. Soc.*, 2016, **138**, 3031–3037.
16 Z. Li, N. Huang, K. H. Lee, Y. Feng, S. Tao, Q. Jiang, Y. Nagao, S. Irle and D. Jiang, *J. Am. Chem. Soc.*, 2018, **140**, 12374–12377.
17 A. Nagai, Z. Guo, X. Feng, S. Jin, X. Chen, X. Ding and D. Jiang, *Nat. Commun.*, 2011, **2**, 536.
18 N. Huang, R. Krishna and D. Jiang, *J. Am. Chem. Soc.*, 2015, **137**, 7079–7082.
19 Q. Lu, Y. Ma, H. Li, X. Guan, Y. Yusran, M. Xue, Q. Fang, Y. Yan, S. Qiu and V. Valtchev, *Angew. Chem., Int. Ed.*, 2018, **57**, 6042–6048.
20 H. Guo, J. Wang, Q. Fang, Y. Zhao, S. Gu, J. Zheng and Y. Yan, *CrystEngComm*, 2017, **19**, 4905–4910.
21 H. S. Xu, S. Y. Ding, W. K. An, H. Wu and W. Wang, *J. Am. Chem. Soc.*, 2016, **138**, 11489–11492.
22 G. Lin, H. Ding, R. Chen, Z. Peng, B. Wang and C. Wang, *J. Am. Chem. Soc.*, 2017, **139**, 8705–8709.
23 R. S. Haszeldine, *Science*, 2009, **325**, 1647–1652.
24 M. E. Boot-Handford, J. C. Abanades, E. J. Anthony, M. J. Blunt, S. Brandani, N. Mac Dowell, J. R. Fernández, M. C. Ferrari, R. Gross and J. P. Hallett, *Energy Environ. Sci.*, 2014, **7**, 130–189.
25 M. Bui, C. S. Adjiman, A. Bardow, E. J. Anthony, A. Boston, S. Brown, P. S. Fennell, S. Fuss, A. Galindo and L. A. Hackett, *Energy Environ. Sci.*, 2018, **11**, 1062–1176.
26 Z. Li, X. Feng, Y. Zou, Y. Zhang, H. Xia, X. Liu and Y. Mu, *Chem. Commun.*, 2014, **50**, 13825–13828.
27 Y. F. Zhi, P. P. Shao, X. Feng, H. Xia, Y. M. Zhang, Z. Shi, Y. Mu and X. M. Liu, *J. Mater. Chem. A*, 2018, **6**, 374–382.
28 Y. Lin, C. Kong, Q. Zhang and L. Chen, *Adv. Energy Mater.*, 2017, **7**, 1601296.
29 R. Dawson, E. Stöckel, J. R. Holst, D. J. Adams and A. I. Cooper, *Energy Environ. Sci.*, 2011, **4**, 4239–4245.
30 R. He, S. Cong, J. Wang, J. Liu and Y. Zhang, *ACS Appl. Mater. Interfaces*, 2019, **11**, 4338–4344.
31 A. K. Sekizkardes, S. Altarawneh, Z. Kahveci, T. İslamoğlu and H. M. El-Kaderi, *Macromolecules*, 2014, **47**, 8328–8334.
32 Q. Chen, M. Luo, P. Hammershøj, D. Zhou, Y. Han, B. W. Laursen, C. G. Yan and B. H. Han, *J. Am. Chem. Soc.*, 2012, **134**, 6084–6087.
33 V. S. P. K. Neti, X. Wu, P. Peng, S. Deng and L. Echegoyen, *RSC Adv.*, 2014, **4**, 9669–9672.
34 X. Zhu, S. M. Mahurin, S. H. An, C. L. Do-Thanh, C. Tian, Y. Li, L. W. Gill, E. W. Hagaman, Z. Bian and J. H. Zhou, *Chem. Commun.*, 2014, **50**, 7933–7936.
35 A. P. Katsoulidis, S. M. Dyar, R. Carmieli, C. D. Malliakas, M. R. Wasielewski and M. G. Kanatzidis, *J. Mater. Chem. A*, 2013, **1**, 10465–10473.
36 M. Grigoras and N. C. Antonoaia, *Eur. Polym. J.*, 2005, **41**, 1079–1089.
37 S. Kandambeth, A. Mallick, B. Lukose, M. V. Mane, T. Heine and R. Banerjee, *J. Am. Chem. Soc.*, 2012, **134**, 19524–19527.
38 S. Dalapati, M. Addicoat, S. Jin, T. Sakurai, J. Gao, H. Xu, S. Irle, S. Seki and D. Jiang, *Nat. Commun.*, 2015, **6**, 7786.
39 Q. Fang, Z. Zhuang, S. Gu, R. B. Kaspar, J. Zheng, J. Wang, S. Qiu and Y. Yan, *Nat. Commun.*, 2014, **5**, 4503.
40 B. Lukose, A. Kuc and T. Heine, *Chem.–Eur. J.*, 2011, **17**, 2388–2392.

41 Z. Li, Y. Zhi, X. Feng, X. Ding, Y. Zou, X. Liu and Y. Mu, *Chem.–Eur. J.*, 2015, **21**, 12079–12084.
42 M. G. Rabbani, A. K. Sekizkardes, Z. Kahveci, T. E. Reich, R. Ding and H. M. El-Kaderi, *Chem.–Eur. J.*, 2013, **19**, 3324–3328.
43 Z. Kahveci, T. Islamoglu, G. A. Shar, R. Ding and H. M. El-Kaderi, *CrystEngComm*, 2013, **15**, 1524–1527.
44 M. G. Rabbani and H. M. El-Kaderi, *Chem. Mater.*, 2012, **24**, 1511–1517.
45 G. Li, B. Zhang, J. Yan and Z. Wang, *Macromolecules*, 2014, **47**, 6664–6670.
46 R. Dawson, D. J. Adams and A. I. Cooper, *Chem. Sci.*, 2011, **2**, 1173–1177.
47 A. L. Myers and J. M. Prausnitz, *AIChE J.*, 1965, **11**, 121–127.
48 H. Wei, S. Chai, N. Hu, Z. Yang, L. Wei and L. Wang, *Chem. Commun.*, 2015, **51**, 12178–12181.
49 H. A. Patel, S. H. Je, J. Park, D. P. Chen, Y. Jung, C. T. Yavuz and A. Coskun, *Nat. Commun.*, 2013, **4**, 1357.
50 Y. Luo, B. Li, W. Wang, K. Wu and B. Tan, *Adv. Mater.*, 2012, **24**, 5703–5707.
51 W. Lu, D. Yuan, J. Sculley, D. Zhao, R. Krishna and H. C. Zhou, *J. Am. Chem. Soc.*, 2011, **133**, 18126–18129.